

CdTe Nanowires studied by Transient Absorption Microscopy

S. S. Lo¹, T. A. Major¹, N. Petchsang¹, L. B. Huang², M. Kuno¹, and G. V. Hartland¹

¹Department of Chemistry and Biochemistry, University of Notre Dame, Notre Dame, Indiana, USA

²Notre Dame Radiation Laboratory, University of Notre Dame, Notre Dame, Indiana, USA

Abstract. Transient absorption measurements were performed on single CdTe nanowires. The traces show fast decays that were assigned to charge carrier trapping at surface states. The observed power dependence suggests the existence of a trap-filling mechanism. Acoustic phonon modes were also observed, which were assigned to breathing modes of the nanowires. Both the fundamental breathing mode and the first overtone were observed, and the dephasing times provide information about how the nanowires interact with their environment.

1 Introduction

Semiconductor nanowires (NW) are promising materials for a variety of applications, such as solar cells [1], lasers[2], logic gates[3] and transport of charge carriers [4]. While there are many examples of NW-based devices, studies on the ultrafast dynamics in these structures are few. Here, we used transient absorption microscopy to study the dynamics of single CdTe NWs at the sub-pico to picoseconds time scale. Single NW experiments provide details that are not accessible in conventional ensemble measurements, such as how dynamics vary between nanowires. These measurements also allow the observation of acoustic vibrational modes of the NWs. The lifetimes of these modes is controlled by radiation of sound waves in the environment, and for our experiments has contributions from both the glass substrate used to support the nanowires, and the surrounding fluid (microscope oil).

2 Results and Discussion

The transient absorption microscopy setup and sample preparation are described in ref. [5]. The ensemble linear and transient absorption (TA) spectra of the CdTe NW sample are shown in Fig. 1A. Here, the two features that are studied in the subsequent single wire TA measurements are indicated: The bleach, B1 (~750 nm), due to state filling of the lowest optical transition, and the induced absorption, A1 (~810 nm), due to the generation of electron-hole pairs by the probe pulse in the presence of charge carriers excited by the pump pulse[6-8]. Representative TEM images of the CdTe NWs are shown in the upper panels of Fig. 1B. These structures have an average width of 29 ± 10 nm (error equals standard deviation) with several microns in length. Single wires are selected in the following way: 1) A branched wire is selected because they are unlikely to form bundles; its scatter image has to be smooth and homogenous with no visible wires surrounding it, as in Fig. 1B lower

This is an Open Access article distributed under the terms of the Creative Commons Attribution License 2.0, which permits unrestricted use, distribution, and reproduction in any medium, provided the original work is properly cited.

left panel. 2) The extinction cross-section of the wire is then measured, and this quantity is used to estimate its radius using a calculated calibration curve[9]; if the estimated radius is similar to those wires of similar morphology observed by TEM, the wire is considered to be a single NW.

TA images and decays are then recorded for the selected wire, which for the current example, are shown in Fig. 1B lower right and Fig. 1C, respectively. Note that the colour of the trace in Fig. 1C corresponds to the decay recorded at the arm denoted by a dashed-circle of the same colour in Fig. 1B lower left panel. The decays were well fitted to a bi-exponential function convolved with a Gaussian; the dominant decay time constants are shown in the figure. The observed short time dynamics are assigned to carrier trapping into surface states, because the decay times are too slow to correspond to electron-phonon coupling[10] and too fast to correspond to carrier diffusion out of the excitation volume.[11] The measured decay times for the NWs are similar to the hole trapping times measured in CdTe quantum dots (QD)[8], and are consistent with the low photoluminescence quantum yields observed in CdTe NWs[12].

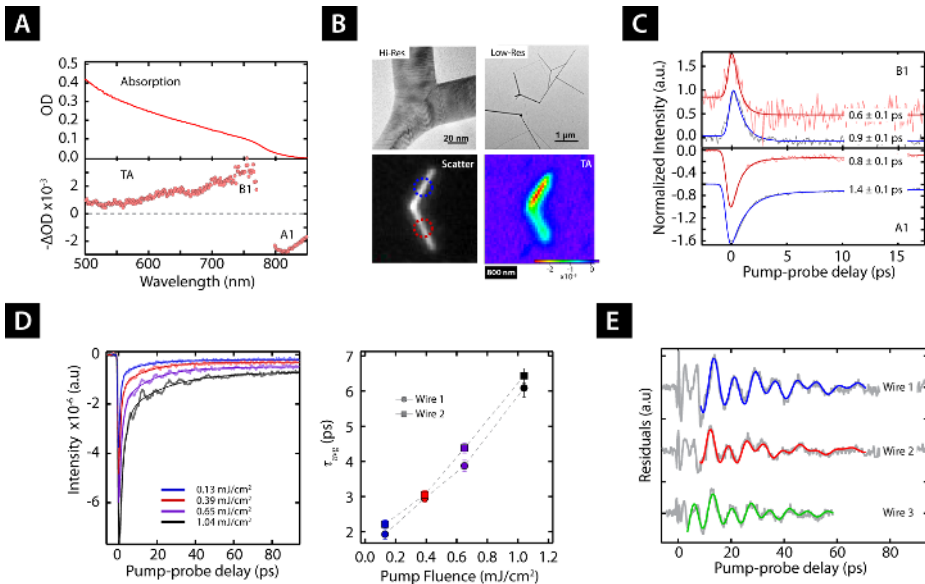


Fig. 1. A) Ensemble absorption and transient absorption (TA) spectra of CdTe NWs. (Reproduced from ref. [5] with permission American Chemical Society 2012) B) Representative TEM, Scatter and TA images of CdTe NWs. (TEM images adapted from ref. [5] with permission American Chemical Society 2012) C) Decays at the Bleach (B1) and induced absorption (A1) feature taken at the two arms (note color coding) of the CdTe NW shown in panel B. D) left panel: Decays recorded at different pump fluence; Right panel: The amplitude weighted average decay time as a function of pump fluence. (Adapted from ref. [5] with permission American Chemical Society 2012) E) Acoustic phonons, grey lines: data, color lines: fit to a damped double cosine function. (Reproduced from ref. [5] with permission American Chemical Society 2012).

The left panel in Figure 1D presents decays recorded at the A1 feature for different pump fluence for a different wire. Both decay time constants were found to increase with increasing pump fluence. This trend is better seen in the right panel of Fig. 1D, where the amplitude weighted average decay time, defined as

$$\tau_{\text{avg}} = \frac{A_1\tau_1 + A_2\tau_2}{A_1 + A_2}, \quad (1)$$

is plotted as a function of pump fluence. Such behaviour is quite unexpected when compared to QDs and CdSe NWs, where an increase in excitation intensity is accompanied by the appearance of a fast time component in the TA trace, that is assigned to Auger relaxation pathways[12]. The observation of slower kinetics for the CdTe NWs is attributed to a trap-filling mechanism, similar to that

invoke in blinking studies of QDs[13] and NWs[14]. Specifically, charge carrier trapping is a second order rate process, which depends on the concentrations of the free charge carriers and the empty trap sites. At high pump fluences the trap sites are filled up, which reduces the rate of trapping[13,14].

Subtracting the bi-exponential fit from the highest pump fluence decay of three different wires results in the traces shown in Fig. 1E. Oscillations are clearly observed, and can be fitted to a damped double cosine function. The fitting procedure yields two periods, whose values are $T_1 = 7.8$, 6.7 and 7.2 ps, and $T_0 = 17.6$, 17.6 and 15.5 ps, for wires 1, 2, and 3 respectively. The time scales of these oscillations are the same order of magnitude as those expected for the breathing modes of the nanowires. The observed phonon modes are assigned to the $n = 0$ (fundamental) and $n = 1$ (first overtone) breathing modes. The measured periods are in good agreement with the results of a continuum model[15], confirming the assignment. In these calculations, the bulk elastic constants of CdTe were used[16], and the NW radius was estimated from the optical absorption cross-section measurements[5]. The damping of the oscillations is due to radiation of sound waves into the surrounding medium[17]. The quality factors measured for the CdTe NWs ($Q = \pi\tau/T$) are similar to those for Ag NWs and nanocubes measured in our laboratory[18]. Calculations of the expected damping times indicate that both the glass substrate and the surrounding microscope oil affect the damping[17,19].

3 Summary and Conclusions

Single CdTe NW were studied using Transient Absorption Microscopy. Fast decays were observed for both bleach and induced absorption features, which are attributed to efficient carrier trapping. The dynamics as a function pump fluence is quite different than those in QDs and CdSe NW, suggesting the influence of a trap-filling mechanism rather than Auger processes. Acoustic phonon modes were also observed. The dephasing times of these modes are similar to those measured for metal nanostructures in our laboratory, and are influenced by interactions with both the glass substrate and the surrounding fluid, which is microscope oil in these experiments.

References

1. Y. Yu, P.V. Kamat, and M. Kuno, *Adv. Funct. Mater.* **20**, 1464 (2010)
2. X. Duan, Y. Huang, R. Agarwal, and C.M. Lieber, *Nature*. **421**, 241 (2003)
3. Y. Huang, X. Duan, Y. Cui, L. Lauhon, K. Kim, and C.M. Lieber, *Science*. **294**, 1313 (2001)
4. A. Dorn, D.B. Strasfeld, D.K. Harris, H.-S. Han, and M.G. Bawendi, *ACS Nano*. **5**, 9028 (2011)
5. S.S. Lo, T.A. Major, N. Petchsang, L.B. Huang, M.K. Kuno and G.V. Hartland, *ACS Nano*. **6**, 5274 (2012)
6. V.I. Klimov, *J. Phys. Chem. B*. **104**, 6112 (2000)
7. P. Kambhampati, *Acc. Chem. Res.* **44**, 1 (2011)
8. Y. Yan, G. Chen, and P.G. Van Patten, *J. Phys. Chem. C*. **115**, 22717 (2011)
9. R. Ruppin, *Opt. Commun.* **211**, 335 (2002)
10. R.P. Prasankumar, P.C. Upadhyaya, and A.J. Taylor, *Phys. Status Solidi b*. **246**, 1973 (2009)
11. B. Segall, R. Halsted, and M. Lorenz, *Phys. Rev.* **129**, 2471 (1963)
12. M. Kuno, O. Ahmad, V. Protasenko, D. Bacinello, T.H. Kosel, *Chem. Mater.* **18**, 5722 (2006).
13. C. Galland, Y. Ghosh, A. Steinbrueck, M. Sykora, J.A. Hollingsworth, V.I. Klimov, and H. Htoon, *Nature*. **479**, 203 (2011)
14. J.J. Glennon, W.E. Buhro, and R.A. Loomis, *J. Phys. Chem. C*. **112**, 4813 (2008)
15. M. Hu, X. Wang, G. Hartland, P. Mulvaney, J. Juste, and J. Sader, *J. Am. Chem. Soc.* **125**, 14925 (2003)
16. G. Simmons, H. Wang, "Single Crystal Elastic Constant and Calculated Aggregate Properties: Handbook," 2nd ed.; The M.I.T. Press: Cambridge, MA, 1971.
17. C. Voisin, N. Del Fatti, D. Christofilos, F. Vallee, *Appl. Surf. Sci.* **164**, 131 (2000)
18. H. Staleva, S.E. Skrabalak, C.R. Carey, T. Kosel, Y. Xia, G.V. Hartland, *Phys. Chem. Chem. Phys.* **11**, 5889 (2009)
19. L. Saviot, C.H. Netting, D.B. Murray, *J. Phys. Chem. B*, **111**, 7457 (2007)